Figure S1

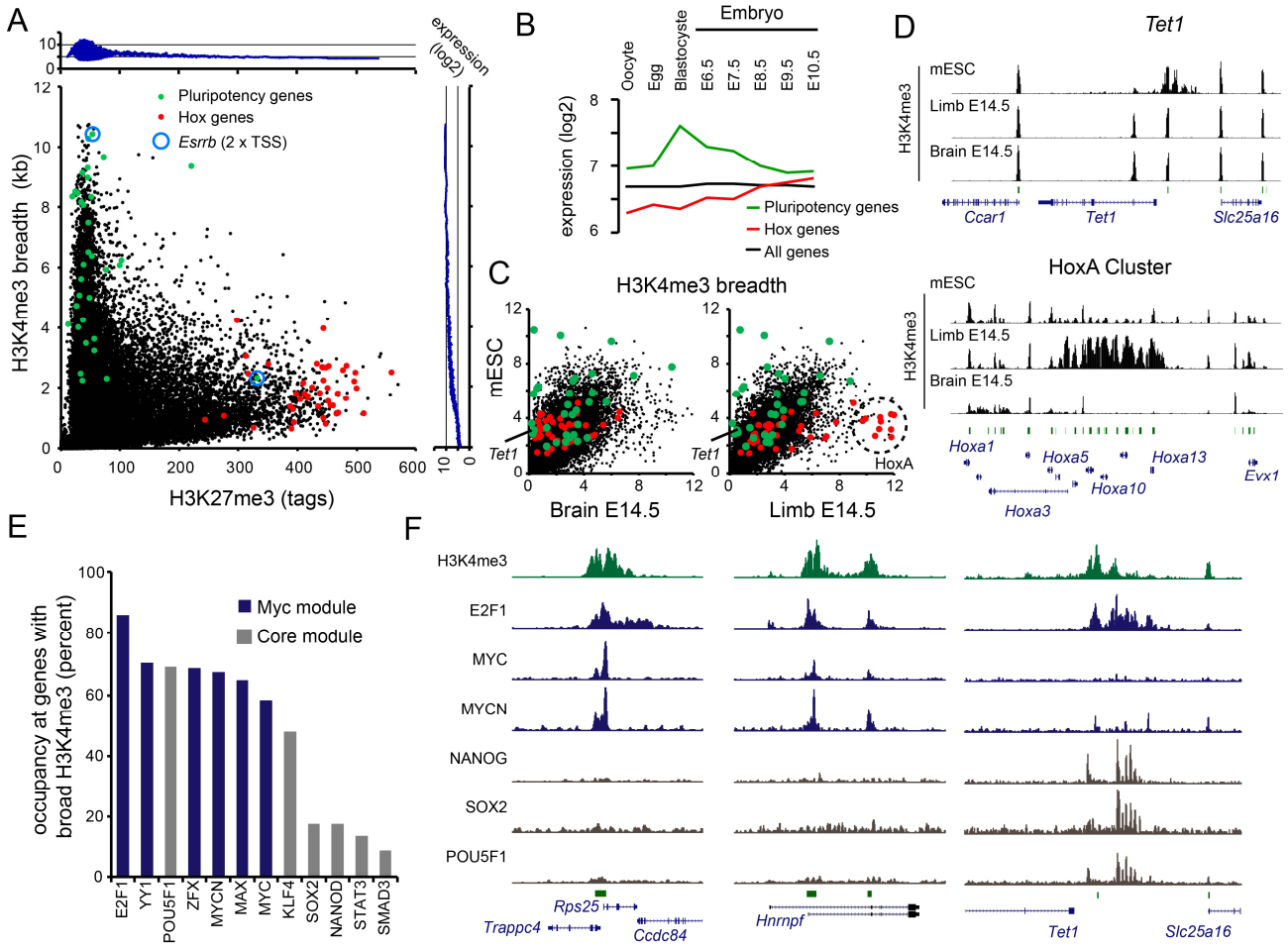

Figure S1: Broad H3K4me3 domains are key regulatory elements in mESCs, related to Figure 1

A) Diagram showing the H3K4me3 breadth and level of H3K27me3 (Mikkelsen et al., 2007) for each gene in mESC. Pluripotency genes and Hox genes are marked by a green or red dot, respectively. The expression curves show a sliding window of 50 datapoints, using data from (De Cegli et al., 2013). The *Esrrb* gene has two transcription start sites, possessing either H3K27me3 or a broad H3K4me3 domain (see also Figure 1B). **B)** Change of the average gene expression during early embryogenesis (Su et al., 2004) of pluripotency, Hox and all genes. **C,D)** H3K4me3 breadth of each gene in mESCs compared to embryonic limb or brain, using data from (Shen et al., 2012). *Tet1* loses H3K4me3 breadth, while the HoxA cluster gains H3K4me3 breadth in the limb. **E)** Occupancy of genes with broad H3K4me3 with members of the Myc (blue) and Core (grey) module. **F)** Three example broad H3K4me3 domains showing the presence of Myc related transcription factors (Kim et al., 2010). Broad H3K4me3 domains at pluripotency genes, such as *Tet1*, are more often occupied by members of the Core module (Whyte et al., 2013).

Figure S2

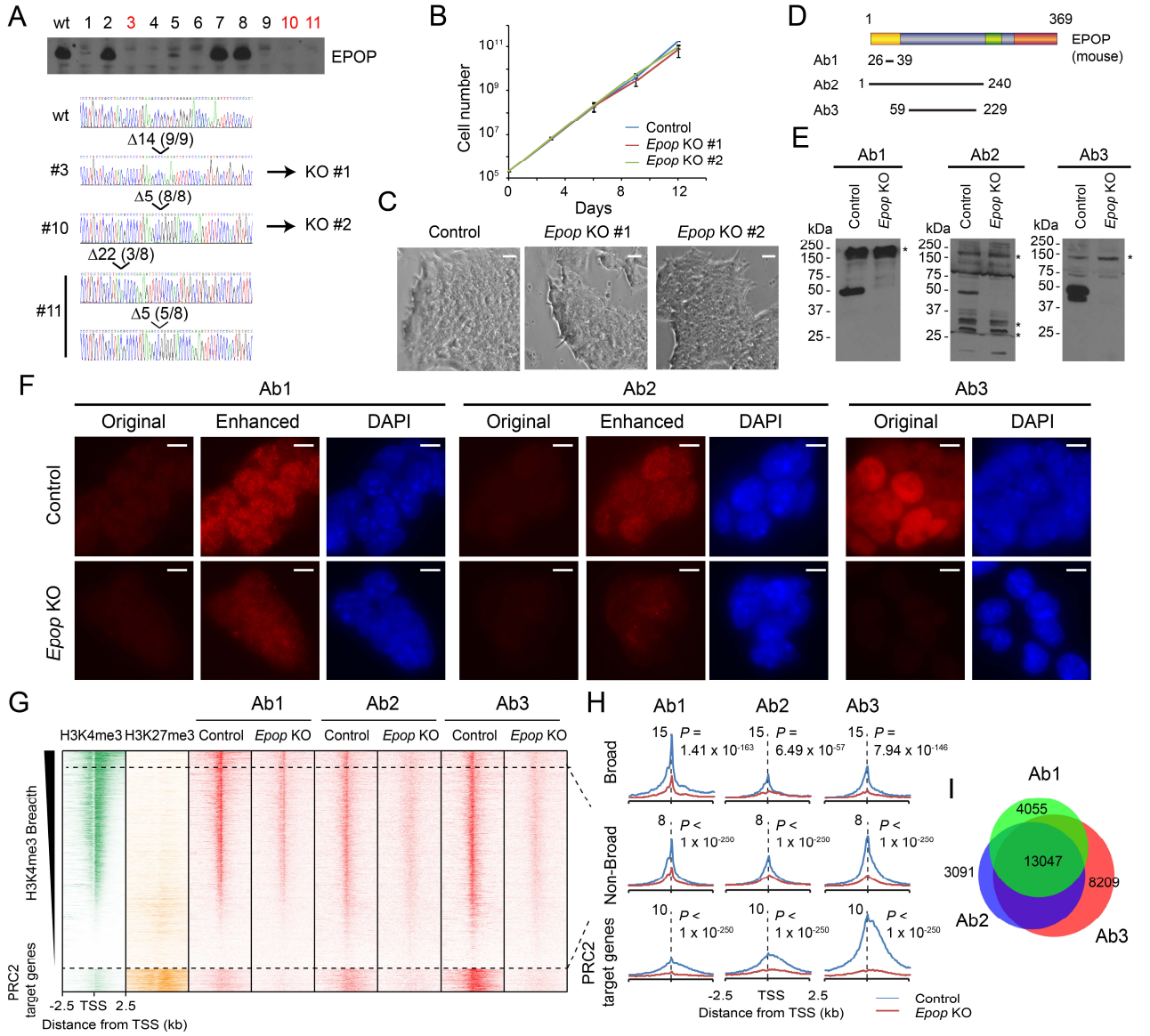

Figure S2: Establishment of *Epop* KO mESCs and antibody validation, related to Figure 1.

A) Western blot showing the screen of several *Epop* CRISPR mESCs knockout clones. Genomic DNA of 3 single cell clones was amplified by PCR, cloned into the pENTR/D vector and sequenced. **B)** Proliferation curves of *Epop* KO clones compared to control cells. Values are mean ± SD of triplicates. **C)** Bright field microscopy of control and *Epop* KO cells. The scale bars indicate 20 µm. **D)** Schematic overview of mouse EPOP pieces used for raising rabbit polyclonal antibodies. Ab1 was made using a peptide, while the antigens for Ab2 and Ab3 were purified as GST-fusion protein. **E)** Western blotting of control or *Epop* KO mESCs using the three antibodies. Asterisks indicate unspecific bands. **F)** Immunofluorescence of control or *Epop* KO mESCs using the three antibodies under identical experimental conditions. For Ab1 and Ab2 the original pictures were computational enhanced. The scale bars indicate 10 µm. **G)** Heatmaps of EPOP ChIP-Seq data obtained from all 3 antibodies in control and *Epop* KO cells. ChIP-Seq data for H3K4me3 and H3K27me3 were used as comparison. **H)** Promoter profiles of the EPOP ChIP-Seq data at genes with and

without broad H3K4me3 domains, as well as PRC2 target genes. The *P*-values were calculated by ANOVA. **I)** Overlap of MACS-called peaks of the three EPOP ChIP-Seq experiments.

Figure S3

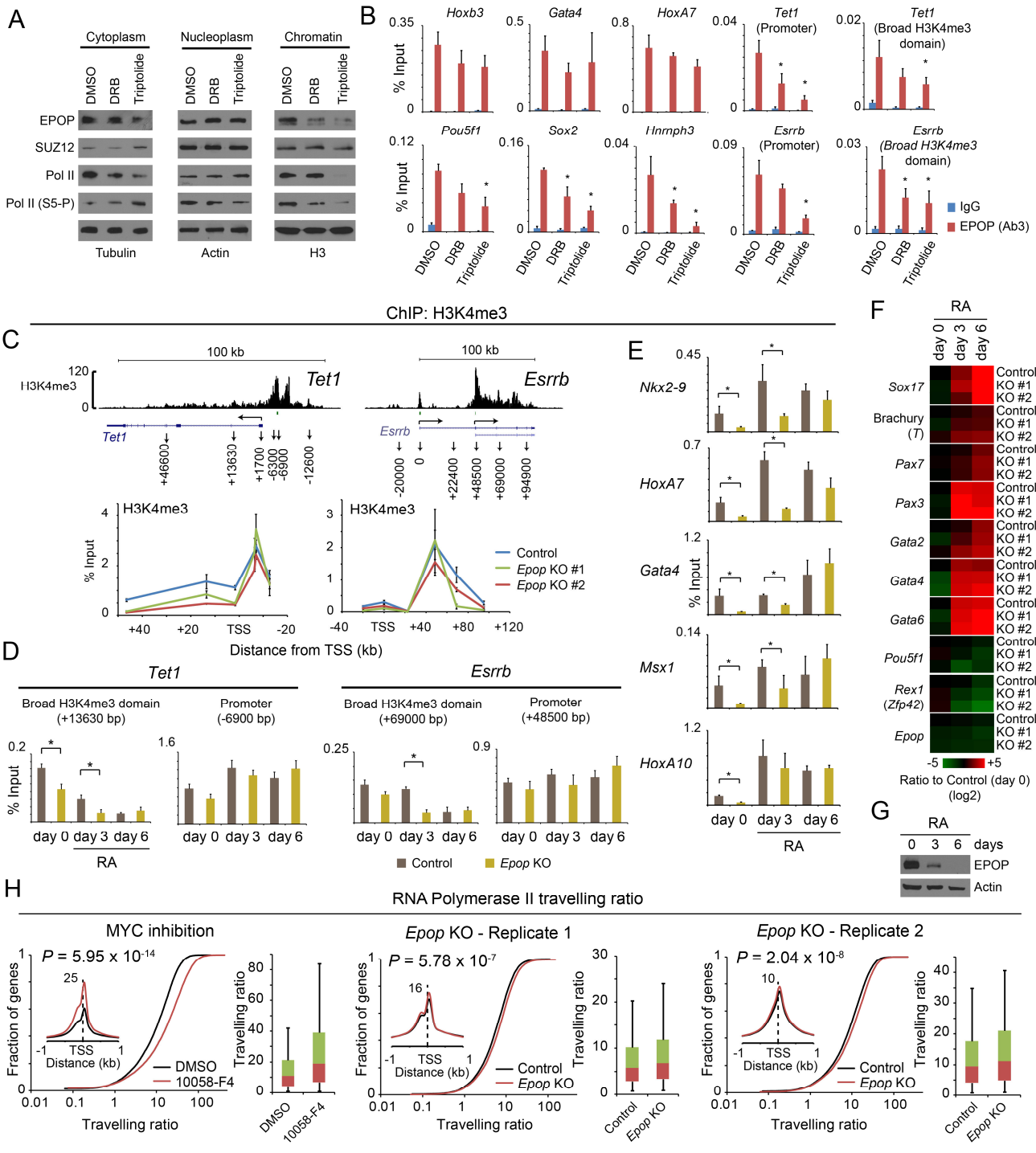

Figure S3. EPOP plays a role at actively transcribed genes, related to Figure 1 and 2.

A) Cellular fractionation of mESCs after treatment with the transcriptional inhibitors DRB or triptolide for 1 hour. Actin, tubulin or H3 is shown as loading control. **B)** EPOP ChIP-qPCR experiments after 1h treatment of wildtype mESCs with DRB and triptolide. Values show mean ± SD of duplicates. (* $p < 0.05$, Student's t-test) **C)** Upper panel: Browser view for H3K4me3 at the *Tet1* and *Esrrb* gene locus, and the primer position for ChIP-qPCR. Lower panel: H3K4me3 ChIP-qPCR for two *Epop* KO clones compared to control cells. The

values indicate mean ± SD of two biological replicates. **D, E)** H3K4me3 ChIP-qPCR at the *Tet and Esrrb* locus, as well as several PRC2 target genes in mESCs upon retinoic acid treatment. Values show mean ± SD of duplicates. (* $p < 0.05$, Student's t-test) **F)** Heatmap for RT-qPCR data showing the change of differentiation markers upon retinoic acid treatments in control and two *Epop* KO cells lines. Values indicate log2 mean expression change of two biological replicates relative to control cells at day 0. **G)** Western blot of EPOP expression during retinoic acid treatment of wildtype mESCs. Actin is shown as loading control. **H)** RNA polymerase II S5 travelling ratio change upon *Epop* KO in comparison to chemical inhibition of MYC (Rahl et al., 2010). The whisker blots represents the distribution of the travelling ratios with lower quartile, median and upper quartile and 5% and 95% whiskers. The *P* values were calculated by a Kolmogorov–Smirnov test.

Figure S4

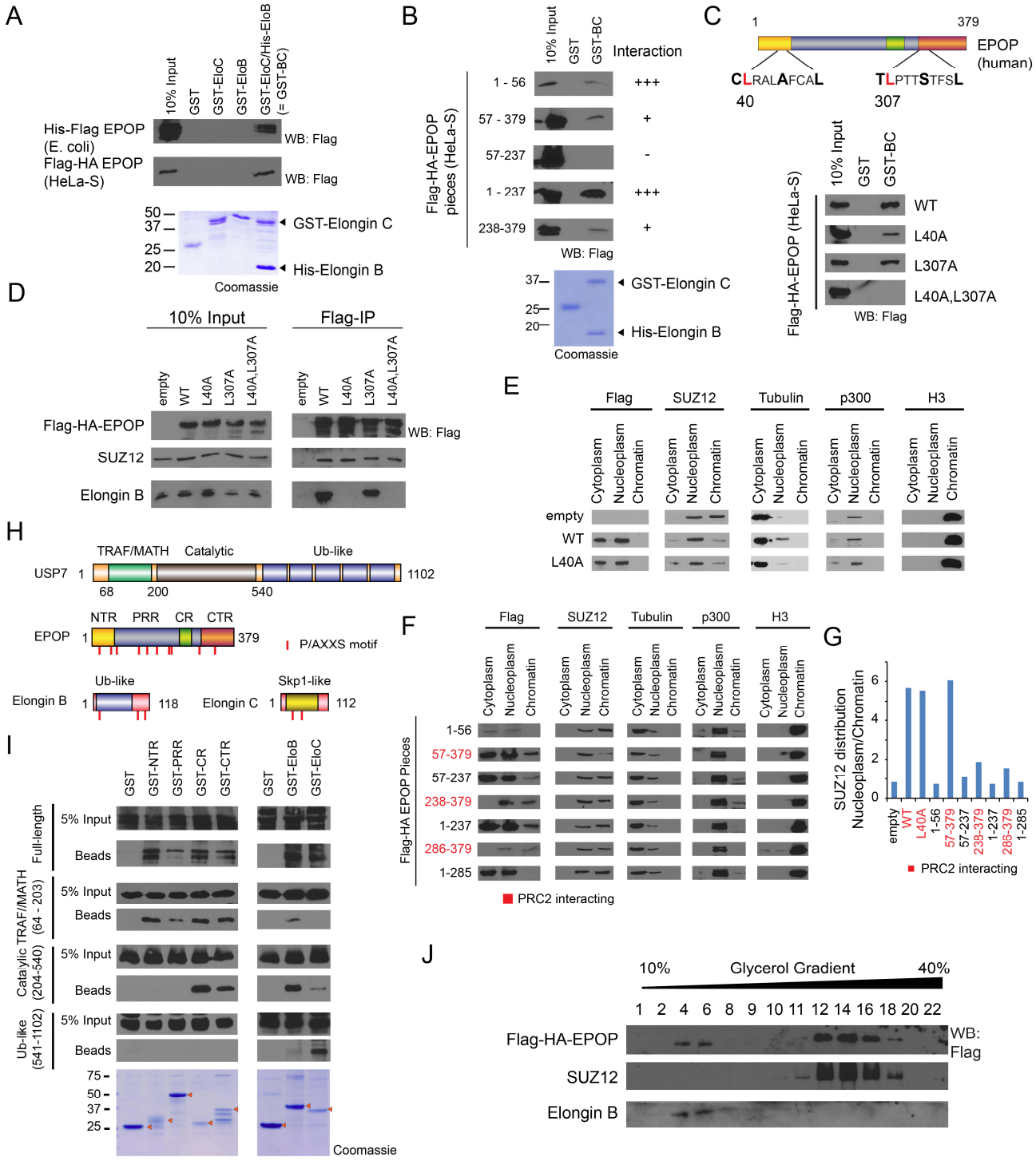

Figure S4: EPOP directly interacts with Elongin BC and USP7, related to Figure 3.
A) Human EPOP either expressed in bacteria or in HeLa-S cells interacts with Elongin BC heterodimer (GST-Elongin C/His-Elongin B = GST-BC). No interaction was observed with GST-Elongin B or GST-Elongin C alone. **B)** GST-Pulldown experiments of pieces of human EPOP expressed in HeLa-S cells using GST-BC as bait**.** The coomassie staining is representative for B) and C). **C)** GST-Pulldown experiment as in B) with EPOP possessing point mutations of the leucines (L40A, L307A) at two putative BC-Boxes. **D)** Semi-

endogenous coimmunoprecipitation of EPOP BC-Box mutants in HeLa-S cells (extended version of Figure 3D). **E)** Cellular fractionation of HeLa-S cells expressing empty vector, wildtype (WT) or L40A mutant EPOP. **F)** Cellular fractionation of HeLa-S cells expressing pieces of EPOP. **G)** Quantification of SUZ12 distribution in E) and F). **H)** Schematic overview of USP7, EPOP and Elongin B and C domain structure and the presence of a P/AXXS motif, which is the typical USP7 binding motif (Sheng et al., 2006). **I)** Coexpression-coupled GST-Pulldown experiment using EPOP pieces or Elongin B and C fused to GST as bait and His-Flag USP7 as prey. PRR = Proline-rich region. The domain structure for EPOP is described in (Liefke and Shi, 2015). A representative coomassie staining is shown. **J)** Western blotting of glycerol gradient fractions of a Flag-purified mouse EPOP complex from mESCs.

Figure S5

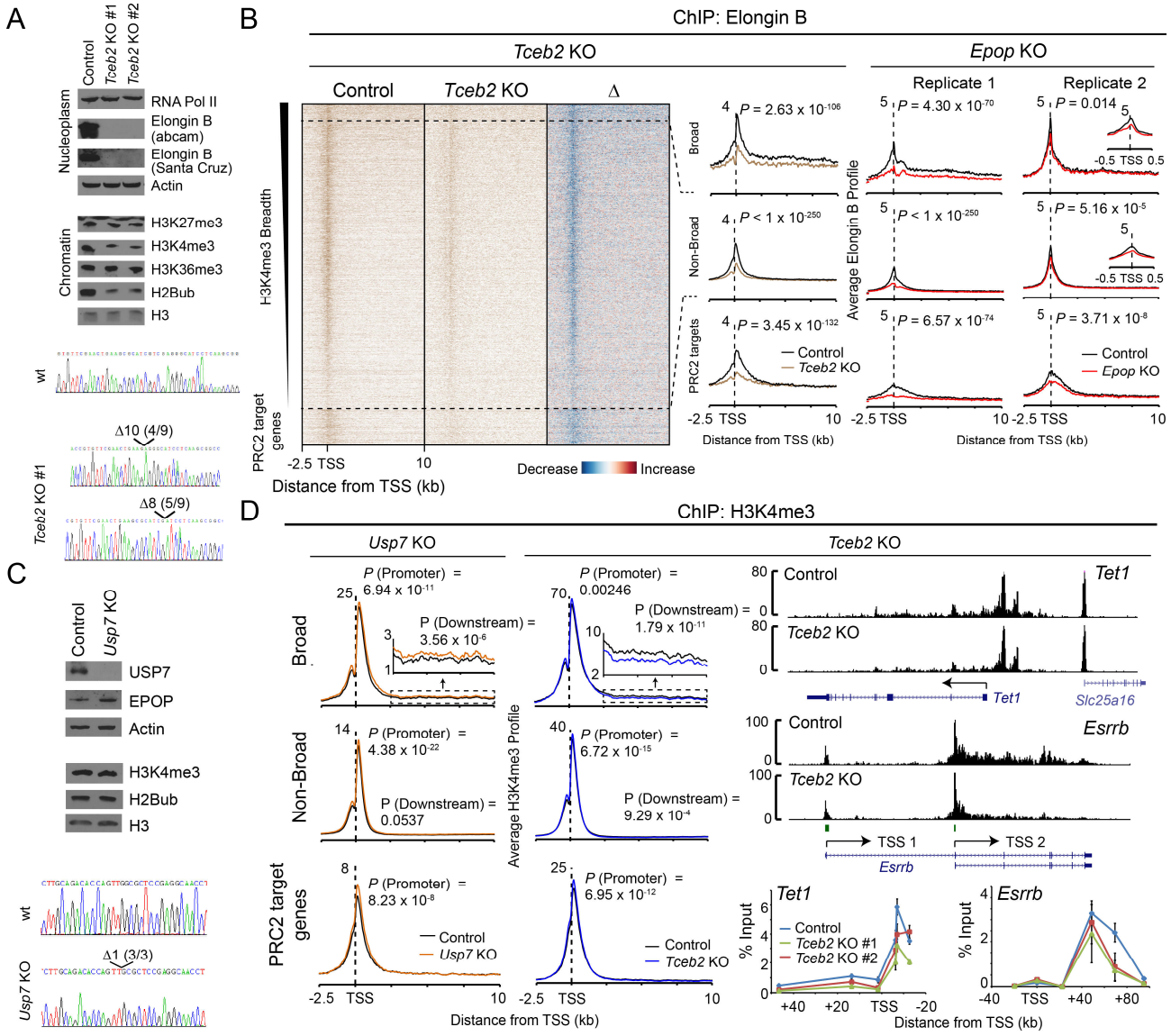

Figure S5. Creation of *Tceb2* and *Usp7* KO mESCs and associated ChIP-Seq experiments, related to Figure 4 and 5.

A) Creation of *Tceb2* KO mESCs using CRISPR/Cas9. Genomic DNA of clone 1 was amplified, incorporated into pENTR/D vector and sequenced. Western blots of proteins and histone marks in those KO cells compared to control cells are shown. Actin or H3 is shown as loading control. **B)** Heatmap and promoter profiles of Elongin B ChIP-Seq in Control versus *Tceb2* and *Epop* KO cells. Two biological replicates are shown for the Elongin B ChIP-Seq in *Epop* KO cells. **C)** Creation of *Usp7* KO cells using CRISPR/Cas9. Genomic DNA was analyzed as described in A). Western blots show level of proteins and histone marks in those KO cells compared to control cells. Actin or H3 is shown as loading control. **D)** Left: H3K4me3 promoter profiles in control versus *Tceb2* or *Usp7* KO cells. Up right: Browser view of H3K4me3 in *Tceb2* KO cells compare to control cells at the *Tet1* and *Esrrb* locus. Down right: H3K4me3 ChIP-qPCR at the *Tet1* and *Esrrb* gene locus with two *Tceb2* KO clones compared to control cells, with primers described in Figure 4C. The values represent mean ± SD of two biological replicates. The *P*-values in B) and D) were calculated by ANOVA.

Figure S6

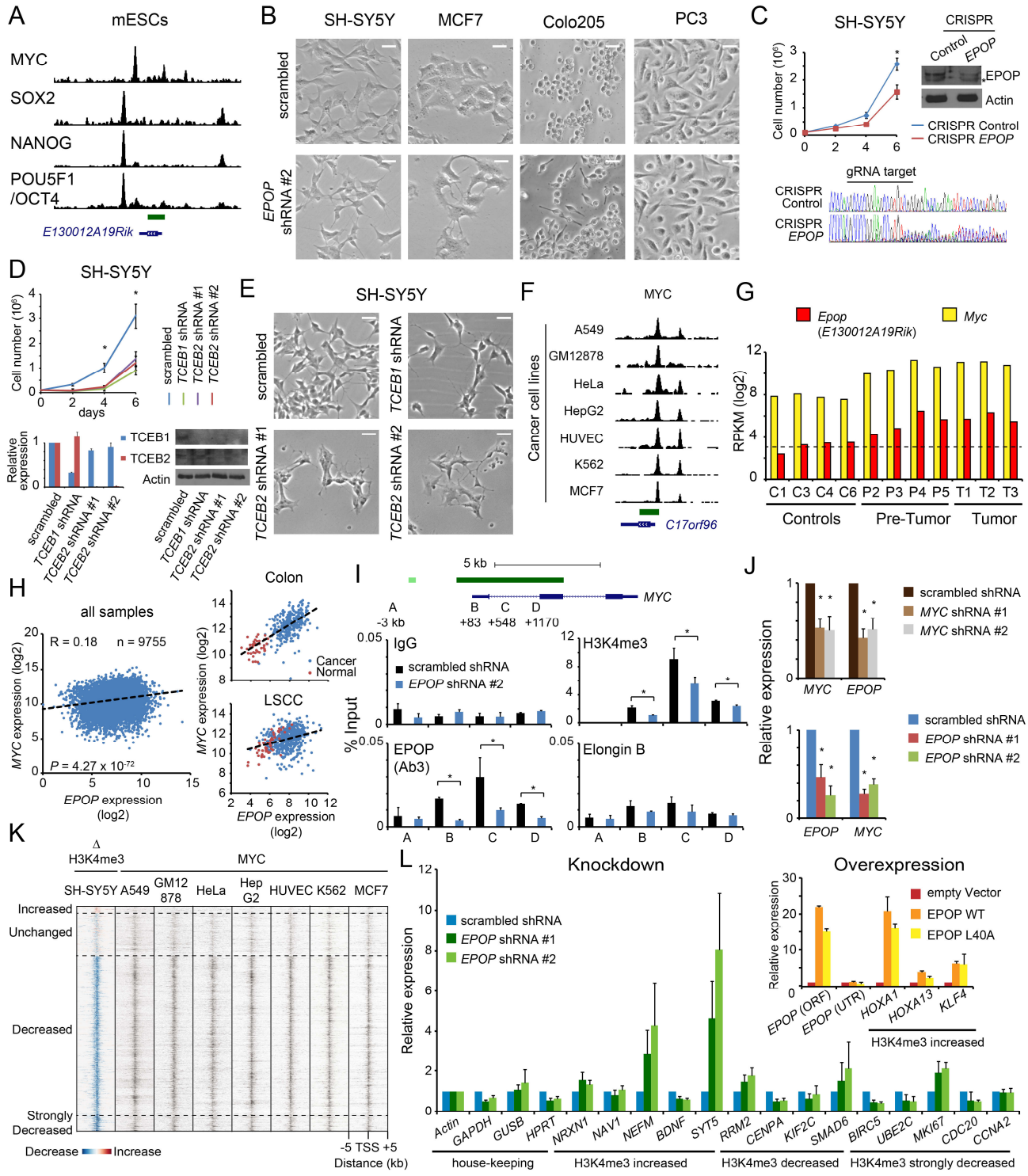

Figure S6: EPOP is involved in cancer cell proliferation, Related to Figure 7.

A) Presence of pluripotency factors (Whyte et al., 2013) (Kim et al., 2010) at the *Epop* (*E130012A19Rik*) gene locus in mESCs. **B)** Bright field microscopy of affected cancer cell lines (Figure 7F) infected with scrambled or shRNA #2 for *EPOP*. Scale bars indicate 20 µm. **C)** Cell proliferation of SH-SY5Y cells upon

infection with *EPOP* CRISPR constructs. The functionality of the CRISPR construct was validated by Western and sequencing of an amplified PCR product. The asterisk in the Western indicates an unspecific band. **D)** Cell proliferation of SH-SY5Y cells upon knockdown of Elongin B and C, validated by qPCR and Western. Actin is shown as loading control in C) and D). **E)** Bright field microscopy of SH-SY5Y cells infected with shRNAs for *TCEB1* and *TCEB2* or control shRNA. The scale bars indicate 20 µm. **F)** Genome browser view of public MYC ChIP-Seq data from cancer cells (ENCODE Project Consortium, 2012) at the *EPOP* (*C17orf96*) gene locus. **G)** Gene expression of *Myc* and *Epop* (*E130012A19Rik*) during mouse lymphomagenesis (Sabo et al., 2014). The dashed line indicates the average *Epop* expression in controls. **H)** Correlation of gene expression of *MYC* and *EPOP* using data from TCGA. The left panel shows all samples and the right panels show Colon (n = 329, R = 0.68, $P = 1.86 \times 10^{-9}$) and Lung Squamous Cell Carcinoma (LSCC) (n = 553, R = 0.31, $P = 5.66 \times 10^{-9}$) as tissue specific examples. The *P*-value was calculated via ANOVA. **I)** ChIP-qPCR in SH-SY5Y cells at the *MYC* locus. The values indicate mean ± SD of duplicates. (* $p < 0.05$, Student's t-test) **J)** RT-qPCR analysis of expression of *EPOP* and *MYC* upon knockdown of *EPOP* and *MYC*. The values represent mean ± SD of duplicates. (* $p < 0.05$, Student's t-test) **K)** Heatmaps of H3K4me3 change in SH-SY5Y cells upon EPOP knockdown compared to presence of MYC from different cancer cells. The heatmaps are sorted after the H3K4me3 changes as described in Figure 7H. **L)** RT-qPCR analysis of several genes with affected H3K4me3 levels in SH-SY5Y cells. The data are presented as mean ± SD of duplicates.

Supplemental Tables

Table S1: Gene ontology analyses, Related to Figure 1, 6, and 7.

Table S2: Used dataset and statistics for the enrichment analysis of chromatin regulators at PRC2 targets genes or genes with broad H3K4me3 domain, Related to Figure 1A.

Table S3: Other ChIP-Seq data used for bioinformatics, Related to Figure 1,2 and 7

Table S4: Used data and statistics for microarray analysis, Related to Figure 6F.

Table S5: Analysis of average gene expression changes in cancer relative to normal tissues, using data from TCGA, Related to Figure 7A.

Table S6: Correlation coefficient of proliferation index versus *EPOP* expression in TCGA cancer samples, Related to Figure 7C.

Table S7: PCR Primers, Related to “Experimental Procedures, ChIP, ChIP-Seq, RNA-Seq, qPCR”.

Extended Experimental Procedures

Cell culture

Retinoic acid treatment of mESCs was performed over 6 days with at concentration of 1 µM. DRB and Triptolide were applied at a concentration of 100 and 10 µM, respectively, for 1 hour. Neuronal monolayer differentiation was performed as described by (Ying et al., 2003). In detail, ES cells were washed twice in PBS and plated onto gelatinized tissue culture flasks at a density of 1×10^4 cells/cm^2 in N2B27 serum-free medium. Medium was changed every day. For the cancer cell proliferation assays 100.000 cells were seeded two days after selection into a 6 well plate and cell numbers were counted every two days. ChIP-Seq, ChIP-qPCR and RT-qPCR experiments in SH-SY5Y were performed two days after selection.

Plasmids

ORFs of wildtype human *EPOP (C17orf96)*, mouse *Epop* (*E130012A19Rik*), and shRNA constructs for mouse *Epop* were obtained as described (Liefke and Shi, 2015). Mutageneses were performed via PCR based cloning strategies. ORFs for human Elongin B and C (*TCEB2* and *TCEB1*) were cloned from cDNA from HeLa-S cells. Lentiviral shRNA constructs for human *EPOP* (shRNA #1: AGCACCGCTGGAGCCTTTAAT, shRNA #2: CGAGGTGCGAGAGGAACAATT), human *TCEB1* (GAAACCAATGAGGTCAATTT) and human *TCEB2* (shRNA #1: GTGTGGCTTCACCAGTCAAAC, shRNA #2: CAGCACGGTGTTCGAACTGAA) were obtained by cloning hairpins, into the pLKO.1 vector. Lentiviral shRNA constructs for *MYC* were obtained from Dharmacon (shRNA #1 TRCN0000039640, shRNA #2: TRCN0000039641). SHC202 (Sigma Aldrich) was used as

shRNA control. CRISPR knockouts were obtained using lentiCRISPRv2 (Addgene #52961) (Sanjana et al., 2014), using following guide RNA targets: *Epop* (*E130012A19Rik*): TACGCCCCTGAAGCCGCGTC, *EPOP* (*C17orf96*): CGCCCCGGAAGCCGTGTCGG, *Tceb2*: GAACTGAAGCGCATCGTCGA, *Usp7*: GGTTGCCTCGGAGCGCCAAC. Single cell clones were obtained via limited dilution and validated by Western blotting and sequencing. A plasmid without functional guide RNA sequences was used as CRISPR control. The CRISPR target sequence was modified by synonymous mutagenesis in mouse EPOP rescue constructs. Rescue and overexpression experiments were performed using untagged EPOP.

Antibodies

Antibody 1 (Ab1) for EPOP was obtained as described (Liefke and Shi, 2015). Antibody 2 (Ab2) was a kind gift of the Luciano Di Croce lab (CRG, Barcelona, Spain). Antibody 3 (Ab3) was derived by injecting rabbits with a purified GST-fusion protein of mouse EPOP containing amino acids 59-229. The antibody was extracted from the obtained serum by affinity purification. Ab3 is available from Active Motif with the catalog number #61753. Experiments in human cancer cells were performed with Ab3. Other used antibodies were SUZ12 (Santa Cruz, sc-46264/sc-271325), p300 (Santa Cruz, sc-585), Tubulin (Sigma, T9026), Actin (abcam, ab3280), Histone H3 (abcam, ab1791), H3K27me3 (Millipore, 07-449), H3K4me3 (Millipore, 04-745), H3K4me2 (Millipore, 07-030), H3K4me1 (abcam, ab8895), H3K36me3 (abcam, 9050), Flag-M2 (Sigma Aldrich, F1804), Flag-M2 beads (Sigma Aldrich, A2220). HA (Covance, MMS-101P), HA Beads (Santa-Cruz, sc-7392), RNA polymerase II (Santa Cruz, sc-899), RNA polymerase II S5 (Covance, MMS-128P; BioLegend, 904001), H2Bub (Cell Signaling, 5546S), Elongin B (abcam, ab168836

(Western/ChIP), Santa Cruz, sc-23407 (Western)), Elongin C (Santa Cruz, sc-1559), POU5F1/OCT4 (Santa-Cruz, sc-5279), Secondary Mouse Anti-Rabbit IgG, Light Chain specific (Jackson Laboratories, 211-032-171)(Western endogenous CoIP), USP7 (Bethyl, A300-033A).

Bioinformatics analyses

ChIP-Seq data were aligned to mouse genome mm9 or human genome hg19, using Bowtie 1.0 (Langmead et al., 2009) with n = 1 and m = 3 as parameters. Normalized and subtraction bigwig files were obtaining using deepTools (Ramirez et al., 2014). Analysis of ChIP-Seq data was done using the Cistrome platform (Liu et al., 2011a) (Liefke and Borggrefe, 2014) or by using custom R scripts for Bioconductor (Gentleman et al., 2004). Significant peaks were called using MACS ($p < 1e-05$). The significance of the ChIP-Seq profiles were evaluated by applying ANOVA on normalized ChIP-seq tag numbers from control and KO cells at regions relative to promoters (H3K4me3-Promoter: -1000 to +1000; H3K4me3-Downstream: +2500 to +10000, H2Bub, USP7: 0 to +1000, EPOP: -1000 to +1000, Elongin B: -500 to +500). The RNA Polymerase II traveling ratios were calculated by dividing the tag density at the promoter region (-250 to +250) by the tag density in the gene body (+1000 to TTS). Only genes with at least 2000 bp length were included into the analysis. The H3K4me3 breadth (in kb, Figure S1A) at a certain gene was determined as the number of 10 bp bins from -2500 to +10000 bp relative to the TSS that contain at least one H3K4me3 tag, divided by 100, using H3K4me3 data from control cells (GSM2027596). The top 1000 genes with broadest H3K4me3 in mESCs were defined as genes with broad H3K4me3 domain (“broad”). The H3K27me3 levels (Figure S1A) were evaluated by counting the H3K27me3 tags from -2500 to +2500 at each promoter, using data from

(Mikkelsen et al., 2007). The enrichment of chromatin regulators (Figure 1A, Table S2) was calculated by dividing the average tag numbers from -2500 to +10000 at broad H3K4me3 possessing genes or PRC2 target genes by the average tag numbers at all genes. RNA-Seq analysis was performed using Tophat and Cufflinks (Trapnell et al., 2012). Microarray data (Table S4) were normalized via RMA using Bioconductor. Gene set enrichment analyses (GSEA) (Subramanian et al., 2005) were performed with standard settings with PRC2 target genes defined as described (Liefke and Shi, 2015). For cancer gene expression analysis (Table S5) the data (PANCAN gene expression, Filename: HiSeqV2_PANCAN-2015-02-15.tgz) were downloaded from the UCSC Cancer Genomics Browser (Cline et al., 2013). Tissues with 5 or less samples were excluded from the analysis. Metastatic or recurrent tumors were considered as cancer samples. The average expression of eleven proliferation associated genes (*BIRC5*, *CCNB1*, *CDC20*, *NUF2*, *CEP55*, *NDC80*, *MKI67*, *PTTG1*, *RRM2*, *TYMS*, *UBE2C*) (Nielsen et al., 2010) of a specific sample was used as proliferation index. The Kaplan-Meier survival plots were obtained as described (Gyorffy et al., 2010) using relapse free survival (RFS) as measure and auto-selected cut-off with following probes: *EPOP* (*C17orf96*): 228066_at, *TCEB1*: 202823_at, *TCEB2*: 200085_s_at. Gene ontology analyses were performed using DAVID or GREAT (Huang da et al., 2009) (McLean et al., 2010).

Complex purification, Glycerol Gradient fractionation and Mass spectrometry

Flag-HA-tagged human or mouse EPOP was expressed after retroviral infection of HeLa-S or mESCs, respectively. Nuclear extract was prepared from the established stable cell lines, and the complex was purified using anti-Flag (M2) conjugated agarose beads (Sigma, A2220), followed by anti-HA conjugated agarose beads (Santa Cruz, sc-7392) by

incubation in TAP buffer (50 mM Tris-HCl pH 7.9, 100 mM KCl, 5 mM MgCl2, 10% glycerol, 0.1% NP-40, 1mM DTT, and protease inhibitors) for 4h and 3 times washing with TAP buffer. Complexes were eluted with Flag or HA peptides, respectively. For glycerol gradient fractionations Flag-purified complexes were layered on an 11-40% glycerol gradient and ultracentrifuged at 55.000 rpm for 10 h. 200µl fractions were subsequently collected manually and analyzed by western blotting, silver staining or mass spectrometry. For mass spectrometry the samples were TCA precipitated and peptides were identified via LC-MS/MS at the Taplin Core facility.

Coimmunoprecipitation experiments and Pulldown experiments

For coimmunoprecipitation experiments whole cell extract were made using CHAPS buffer (Tris 50 mM pH 7.8, 350 mM NaCl, 1 mDTT, 10 mM CHAPS) and samples were incubated with the appropriate antibody for 4 h at 4 °C and precipitated using protein A beads. After washing the beads with CHAPS buffer, the precipitated proteins were visualized by Western blotting.

For pulldown experiments using Elongin BC dimers as bait, GST-Elongin C and His-Elongin B were coexpressed in BL21 cells and batch purified before the experiments. Bacterial expressed His-Flag-EPOP was expressed in BL21 cells at 16C with 0.1 M IPTG and purified using Ni-NTA beads. For other experiment Flag-HA constructs of the respective human EPOP piece or mutant were expressed in HeLa-S cells. Whole cell extracts were made using CHAPS buffer and incubated with glutathione-beads immobilized GST-Elongin BC or GST alone for 2 hours and washed three times with CHAPS buffer. Bound proteins were visualized by Western blotting using a Flag antibody.

Coexpression coupled GST-Pulldown experiments (Figure S4I) were performed as described (Liefke and Shi, 2015) with following modifications: Protein were coexpressed with 0.1M IPTG in BL21 cells cultured at 20 °C. For washing a CHAPS buffer containing 1 M NaCl was used. GST-fusion proteins of human EPOP (NTR: 1-56, PRR: 57-237, CR: 238-285, CTR: 286-379), Elongin B and C were used as bait and His-Flag-tagged full-length or specific domains of human USP7 as prey.

Cellular Fractionation

Cellular fractionations were performed using “Subcellular Protein Fractionation Kit for Cultured Cells“ (Pierce, #78840) according to manufacturer’s instructions, followed by Western blotting. A 1:3 sample dilution was used for Western blotting to detect histone modifications. Protein levels were quantified using Photoshop.

Statistical analysis

Statistical analyses were performed using unpaired Student’s t-tests (qPCRs, comparison of gene groups), Kolmogorov–Smirnov tests (Travelling ratios), ANOVA (Regression, Significance of ChIP-Seq data), hypergeometric tests or were calculated by the GSEA, GREAT, DAVID or Cistrome tools.

Supplemental References

Ballare, C., Lange, M., Lapinaite, A., Martin, G.M., Morey, L., Pascual, G., Liefke, R., Simon, B., Shi, Y., Gozani, O*., et al.* (2012). Phf19 links methylated Lys36 of histone H3 to regulation of Polycomb activity. Nat Struct Mol Biol *19*, 1257-1265.

Beshiri, M.L., Holmes, K.B., Richter, W.F., Hess, S., Islam, A.B., Yan, Q., Plante, L., Litovchick, L., Gevry, N., Lopez-Bigas, N*., et al.* (2012). Coordinated repression of cell cycle genes by KDM5A and E2F4 during differentiation. Proc Natl Acad Sci U S A *109*, 18499-18504.

Blackledge, N.P., Zhou, J.C., Tolstorukov, M.Y., Farcas, A.M., Park, P.J., and Klose, R.J. (2010). CpG islands recruit a histone H3 lysine 36 demethylase. Mol Cell *38*, 179-190.

Chen, X., Xu, H., Yuan, P., Fang, F., Huss, M., Vega, V.B., Wong, E., Orlov, Y.L., Zhang, W., Jiang, J*., et al.* (2008). Integration of external signaling pathways with the core transcriptional network in embryonic stem cells. Cell *133*, 1106-1117.

Cline, M.S., Craft, B., Swatloski, T., Goldman, M., Ma, S., Haussler, D., and Zhu, J. (2013). Exploring TCGA Pan-Cancer data at the UCSC Cancer Genomics Browser. Sci Rep *3*, 2652.

Dan, J., Liu, Y., Liu, N., Chiourea, M., Okuka, M., Wu, T., Ye, X., Mou, C., Wang, L., Yin, Y*., et al.* (2014). Rif1 maintains telomere length homeostasis of ESCs by mediating heterochromatin silencing. Dev Cell *29*, 7-19.

Das, P.P., Shao, Z., Beyaz, S., Apostolou, E., Pinello, L., De Los Angeles, A., O'Brien, K., Atsma, J.M., Fujiwara, Y., Nguyen, M*., et al.* (2014). Distinct and combinatorial functions of Jmjd2b/Kdm4b and Jmjd2c/Kdm4c in mouse embryonic stem cell identity. Mol Cell *53*, 32-48.

Denissov, S., Hofemeister, H., Marks, H., Kranz, A., Ciotta, G., Singh, S., Anastassiadis, K., Stunnenberg, H.G., and Stewart, A.F. (2014). Mll2 is required for H3K4 trimethylation on bivalent promoters in embryonic stem cells, whereas Mll1 is redundant. Development *141*, 526-537.

Ding, L., Paszkowski-Rogacz, M., Nitzsche, A., Slabicki, M.M., Heninger, A.K., de Vries, I., Kittler, R., Junqueira, M., Shevchenko, A., Schulz, H*., et al.* (2009). A genome-scale RNAi screen for Oct4 modulators defines a role of the Paf1 complex for embryonic stem cell identity. Cell Stem Cell *4*, 403-415.

ENCODE Project Consortium (2012). An integrated encyclopedia of DNA elements in the human genome. Nature *489*, 57-74.

Gao, X., Tate, P., Hu, P., Tjian, R., Skarnes, W.C., and Wang, Z. (2008). ES cell pluripotency and germ-layer formation require the SWI/SNF chromatin remodeling component BAF250a. Proc Natl Acad Sci U S A *105*, 6656-6661.

Gentleman, R.C., Carey, V.J., Bates, D.M., Bolstad, B., Dettling, M., Dudoit, S., Ellis, B., Gautier, L., Ge, Y., Gentry, J*., et al.* (2004). Bioconductor: open software development for computational biology and bioinformatics. Genome Biol *5*, R80.

Grijzenhout, A., Godwin, J., Koseki, H., Gdula, M.R., Szumska, D., McGouran, J.F., Bhattacharya, S., Kessler, B.M., Brockdorff, N., and Cooper, S. (2016). Functional analysis of AEBP2, a PRC2 Polycomb protein, reveals a Trithorax phenotype in embryonic development and in ESCs. Development *143*, 2716-2723.

Gyorffy, B., Lanczky, A., Eklund, A.C., Denkert, C., Budczies, J., Li, Q., and Szallasi, Z. (2010). An online survival analysis tool to rapidly assess the effect of 22,277 genes on breast cancer prognosis using microarray data of 1,809 patients. Breast Cancer Res Treat *123*, 725-731.

Handoko, L., Xu, H., Li, G., Ngan, C.Y., Chew, E., Schnapp, M., Lee, C.W., Ye, C., Ping, J.L., Mulawadi, F*., et al.* (2011). CTCF-mediated functional chromatin interactome in pluripotent cells. Nat Genet *43*, 630-638.

He, J., Shen, L., Wan, M., Taranova, O., Wu, H., and Zhang, Y. (2013). Kdm2b maintains murine embryonic stem cell status by recruiting PRC1 complex to CpG islands of developmental genes. Nat Cell Biol *15*, 373-384.

Ho, L., Ronan, J.L., Wu, J., Staahl, B.T., Chen, L., Kuo, A., Lessard, J., Nesvizhskii, A.I., Ranish, J., and Crabtree, G.R. (2009). An embryonic stem cell chromatin remodeling complex, esBAF, is essential for embryonic stem cell self-renewal and pluripotency. Proc Natl Acad Sci U S A *106*, 5181-5186.

Huang da, W., Sherman, B.T., and Lempicki, R.A. (2009). Systematic and integrative analysis of large gene lists using DAVID bioinformatics resources. Nat Protoc *4*, 44-57.
Jiang, H., Shukla, A., Wang, X., Chen, W.Y., Bernstein, B.E., and Roeder, R.G. (2011). Role for Dpy-30 in ES cell-fate specification by regulation of H3K4 methylation within bivalent domains. Cell *144*, 513-525.
Kagey, M.H., Newman, J.J., Bilodeau, S., Zhan, Y., Orlando, D.A., van Berkum, N.L., Ebmeier, C.C., Goossens, J., Rahl, P.B., Levine, S.S.*, et al.* (2010). Mediator and cohesin connect gene expression and chromatin architecture. Nature *467*, 430-435.
Kaneko, S., Son, J., Shen, S.S., Reinberg, D., and Bonasio, R. (2013). PRC2 binds active promoters and contacts nascent RNAs in embryonic stem cells. Nat Struct Mol Biol *20*, 1258-1264.
Kidder, B.L., Hu, G., and Zhao, K. (2014). KDM5B focuses H3K4 methylation near promoters and enhancers during embryonic stem cell self-renewal and differentiation. Genome Biol *15*, R32.
Kim, J., Woo, A.J., Chu, J., Snow, J.W., Fujiwara, Y., Kim, C.G., Cantor, A.B., and Orkin, S.H. (2010). A Myc network accounts for similarities between embryonic stem and cancer cell transcription programs. Cell *143*, 313-324.
Krepelova, A., Neri, F., Maldotti, M., Rapelli, S., and Oliviero, S. (2014). Myc and max genome-wide binding sites analysis links the Myc regulatory network with the polycomb and the core pluripotency networks in mouse embryonic stem cells. PLoS One *9*, e88933.
Langmead, B., Trapnell, C., Pop, M., and Salzberg, S.L. (2009). Ultrafast and memory-efficient alignment of short DNA sequences to the human genome. Genome Biol *10*, R25.
Leeb, M., Pasini, D., Novatchkova, M., Jaritz, M., Helin, K., and Wutz, A. (2010). Polycomb complexes act redundantly to repress genomic repeats and genes. Genes Dev *24*, 265-276.
Li, G., Margueron, R., Ku, M., Chambon, P., Bernstein, B.E., and Reinberg, D. (2010). Jarid2 and PRC2, partners in regulating gene expression. Genes Dev *24*, 368-380.
Li, X., Li, L., Pandey, R., Byun, J.S., Gardner, K., Qin, Z., and Dou, Y. (2012). The histone acetyltransferase MOF is a key regulator of the embryonic stem cell core transcriptional network. Cell Stem Cell *11*, 163-178.
Lin, C., Garruss, A.S., Luo, Z., Guo, F., and Shilatifard, A. (2013). The RNA Pol II elongation factor Ell3 marks enhancers in ES cells and primes future gene activation. Cell *152*, 144-156.
Lin, W., Cao, J., Liu, J., Beshiri, M.L., Fujiwara, Y., Francis, J., Cherniack, A.D., Geisen, C., Blair, L.P., Zou, M.R.*, et al.* (2011b). Loss of the retinoblastoma binding protein 2 (RBP2) histone demethylase suppresses tumorigenesis in mice lacking Rb1 or Men1. Proc Natl Acad Sci U S A *108*, 13379-13386.
Liu, T., Ortiz, J.A., Taing, L., Meyer, C.A., Lee, B., Zhang, Y., Shin, H., Wong, S.S., Ma, J., Lei, Y.*, et al.* (2011a). Cistrome: an integrative platform for transcriptional regulation studies. Genome Biol *12*, R83.
Liu, Z., Scannell, D.R., Eisen, M.B., and Tjian, R. (2011b). Control of embryonic stem cell lineage commitment by core promoter factor, TAF3. Cell *146*, 720-731.
Lohmann, F., Loureiro, J., Su, H., Fang, Q., Lei, H., Lewis, T., Yang, Y., Labow, M., Li, E., Chen, T., and Kadam, S. (2010). KMT1E mediated H3K9 methylation is required for the maintenance of embryonic stem cells by repressing trophectoderm differentiation. Stem Cells *28*, 201-212.
Mattout, A., Aaronson, Y., Sailaja, B.S., Raghu Ram, E.V., Harikumar, A., Mallm, J.P., Sim, K.H., Nissim-Rafinia, M., Supper, E., Singh, P.B.*, et al.* (2015). Heterochromatin Protein 1beta (HP1beta) has distinct functions and distinct nuclear distribution in pluripotent versus differentiated cells. Genome Biol *16*, 213.
McLean, C.Y., Bristor, D., Hiller, M., Clarke, S.L., Schaar, B.T., Lowe, C.B., Wenger, A.M., and Bejerano, G. (2010). GREAT improves functional interpretation of cis-regulatory regions. Nat Biotechnol *28*, 495-501.
Mikkelsen, T.S., Ku, M., Jaffe, D.B., Issac, B., Lieberman, E., Giannoukos, G., Alvarez, P., Brockman, W., Kim, T.K., Koche, R.P.*, et al.* (2007). Genome-wide maps of chromatin state in pluripotent and lineage-committed cells. Nature *448*, 553-560.
Miyazaki, H., Higashimoto, K., Yada, Y., Endo, T.A., Sharif, J., Komori, T., Matsuda, M., Koseki, Y., Nakayama, M., Soejima, H.*, et al.* (2013). Ash1l methylates Lys36 of histone H3 independently of transcriptional elongation to counteract polycomb silencing. PLoS Genet *9*, e1003897.

Morey, L., Aloia, L., Cozzuto, L., Benitah, S.A., and Di Croce, L. (2013). RYBP and Cbx7 define specific biological functions of polycomb complexes in mouse embryonic stem cells. Cell Rep *3*, 60-69.
Morey, L., Santanach, A., Blanco, E., Aloia, L., Nora, E.P., Bruneau, B.G., and Di Croce, L. (2015). Polycomb Regulates Mesoderm Cell Fate-Specification in Embryonic Stem Cells through Activation and Repression Mechanisms. Cell Stem Cell *17*, 300-315.
Mullen, A.C., Orlando, D.A., Newman, J.J., Loven, J., Kumar, R.M., Bilodeau, S., Reddy, J., Guenther, M.G., DeKoter, R.P., and Young, R.A. (2011). Master transcription factors determine cell-type-specific responses to TGF-beta signaling. Cell *147*, 565-576.
Nielsen, T.O., Parker, J.S., Leung, S., Voduc, D., Ebbert, M., Vickery, T., Davies, S.R., Snider, J., Stijleman, I.J., Reed, J*., et al.* (2010). A comparison of PAM50 intrinsic subtyping with immunohistochemistry and clinical prognostic factors in tamoxifen-treated estrogen receptor-positive breast cancer. Clin Cancer Res *16*, 5222-5232.
Outchkourov, N.S., Muino, J.M., Kaufmann, K., van Ijcken, W.F., Groot Koerkamp, M.J., van Leenen, D., de Graaf, P., Holstege, F.C., Grosveld, F.G., and Timmers, H.T. (2013). Balancing of histone H3K4 methylation states by the Kdm5c/SMCX histone demethylase modulates promoter and enhancer function. Cell Rep *3*, 1071-1079.
Pasini, D., Bracken, A.P., Hansen, J.B., Capillo, M., and Helin, K. (2007). The polycomb group protein Suz12 is required for embryonic stem cell differentiation. Mol Cell Biol *27*, 3769-3779.
Pedersen, M.T., Agger, K., Laugesen, A., Johansen, J.V., Cloos, P.A., Christensen, J., and Helin, K. (2014). The demethylase JMJD2C localizes to H3K4me3-positive transcription start sites and is dispensable for embryonic development. Mol Cell Biol *34*, 1031-1045.
Rais, Y., Zviran, A., Geula, S., Gafni, O., Chomsky, E., Viukov, S., Mansour, A.A., Caspi, I., Krupalnik, V., Zerbib, M*., et al.* (2013). Deterministic direct reprogramming of somatic cells to pluripotency. Nature *502*, 65-70.
Ramirez, F., Dundar, F., Diehl, S., Gruning, B.A., and Manke, T. (2014). deepTools: a flexible platform for exploring deep-sequencing data. Nucleic Acids Res *42*, W187-191.
Ravens, S., Fournier, M., Ye, T., Stierle, M., Dembele, D., Chavant, V., and Tora, L. (2014). Mof-associated complexes have overlapping and unique roles in regulating pluripotency in embryonic stem cells and during differentiation. Elife *3*.
Ravens, S., Yu, C., Ye, T., Stierle, M., and Tora, L. (2015). Tip60 complex binds to active Pol II promoters and a subset of enhancers and co-regulates the c-Myc network in mouse embryonic stem cells. Epigenetics Chromatin *8*, 45.
Schmitz, S.U., Albert, M., Malatesta, M., Morey, L., Johansen, J.V., Bak, M., Tommerup, N., Abarrategui, I., and Helin, K. (2011). Jarid1b targets genes regulating development and is involved in neural differentiation. EMBO J *30*, 4586-4600.
Schnetz, M.P., Handoko, L., Akhtar-Zaidi, B., Bartels, C.F., Pereira, C.F., Fisher, A.G., Adams, D.J., Flicek, P., Crawford, G.E., Laframboise, T*., et al.* (2010). CHD7 targets active gene enhancer elements to modulate ES cell-specific gene expression. PLoS Genet *6*, e1001023.
Shen, X., Kim, W., Fujiwara, Y., Simon, M.D., Liu, Y., Mysliwiec, M.R., Yuan, G.C., Lee, Y., and Orkin, S.H. (2009). Jumonji modulates polycomb activity and self-renewal versus differentiation of stem cells. Cell *139*, 1303-1314.
Shen, X., Liu, Y., Hsu, Y.J., Fujiwara, Y., Kim, J., Mao, X., Yuan, G.C., and Orkin, S.H. (2008). EZH1 mediates methylation on histone H3 lysine 27 and complements EZH2 in maintaining stem cell identity and executing pluripotency. Mol Cell *32*, 491-502.
Shen, Y., Yue, F., McCleary, D.F., Ye, Z., Edsall, L., Kuan, S., Wagner, U., Dixon, J., Lee, L., Lobanenkov, V.V., and Ren, B. (2012). A map of the cis-regulatory sequences in the mouse genome. Nature *488*, 116-120.
Sheng, Y., Saridakis, V., Sarkari, F., Duan, S., Wu, T., Arrowsmith, C.H., and Frappier, L. (2006). Molecular recognition of p53 and MDM2 by USP7/HAUSP. Nat Struct Mol Biol *13*, 285-291.

Smith, E.R., Lin, C., Garrett, A.S., Thornton, J., Mohaghegh, N., Hu, D., Jackson, J., Saraf, A., Swanson, S.K., Seidel, C.*, et al.* (2011). The little elongation complex regulates small nuclear RNA transcription. Mol Cell *44*, 954-965.
Sridharan, R., Gonzales-Cope, M., Chronis, C., Bonora, G., McKee, R., Huang, C., Patel, S., Lopez, D., Mishra, N., Pellegrini, M.*, et al.* (2013). Proteomic and genomic approaches reveal critical functions of H3K9 methylation and heterochromatin protein-1gamma in reprogramming to pluripotency. Nat Cell Biol *15*, 872-882.
Su, A.I., Wiltshire, T., Batalov, S., Lapp, H., Ching, K.A., Block, D., Zhang, J., Soden, R., Hayakawa, M., Kreiman, G.*, et al.* (2004). A gene atlas of the mouse and human protein-encoding transcriptomes. Proc Natl Acad Sci U S A *101*, 6062-6067.
Subramanian, A., Tamayo, P., Mootha, V.K., Mukherjee, S., Ebert, B.L., Gillette, M.A., Paulovich, A., Pomeroy, S.L., Golub, T.R., Lander, E.S., and Mesirov, J.P. (2005). Gene set enrichment analysis: a knowledge-based approach for interpreting genome-wide expression profiles. Proc Natl Acad Sci U S A *102*, 15545-15550.
Surface, L.E., Fields, P.A., Subramanian, V., Behmer, R., Udeshi, N., Peach, S.E., Carr, S.A., Jaffe, J.D., and Boyer, L.A. (2016). H2A.Z.1 Monoubiquitylation Antagonizes BRD2 to Maintain Poised Chromatin in ESCs. Cell Rep *14*, 1142-1155.
Sussman, R.T., Stanek, T.J., Esteso, P., Gearhart, J.D., Knudsen, K.E., and McMahon, S.B. (2013). The epigenetic modifier ubiquitin-specific protease 22 (USP22) regulates embryonic stem cell differentiation via transcriptional repression of sex-determining region Y-box 2 (SOX2). J Biol Chem *288*, 24234-24246.
Tee, W.W., Shen, S.S., Oksuz, O., Narendra, V., and Reinberg, D. (2014). Erk1/2 activity promotes chromatin features and RNAPII phosphorylation at developmental promoters in mouse ESCs. Cell *156*, 678-690.
Trapnell, C., Roberts, A., Goff, L., Pertea, G., Kim, D., Kelley, D.R., Pimentel, H., Salzberg, S.L., Rinn, J.L., and Pachter, L. (2012). Differential gene and transcript expression analysis of RNA-seq experiments with TopHat and Cufflinks. Nat Protoc *7*, 562-578.
Vella, P., Barozzi, I., Cuomo, A., Bonaldi, T., and Pasini, D. (2012). Yin Yang 1 extends the Myc-related transcription factors network in embryonic stem cells. Nucleic Acids Res *40*, 3403-3418.
Vella, P., Scelfo, A., Jammula, S., Chiacchiera, F., Williams, K., Cuomo, A., Roberto, A., Christensen, J., Bonaldi, T., Helin, K., and Pasini, D. (2013). Tet proteins connect the O-linked N-acetylglucosamine transferase Ogt to chromatin in embryonic stem cells. Mol Cell *49*, 645-656.
Walker, E., Chang, W.Y., Hunkapiller, J., Cagney, G., Garcha, K., Torchia, J., Krogan, N.J., Reiter, J.F., and Stanford, W.L. (2010). Polycomb-like 2 associates with PRC2 and regulates transcriptional networks during mouse embryonic stem cell self-renewal and differentiation. Cell Stem Cell *6*, 153-166.
Wang, L., Du, Y., Ward, J.M., Shimbo, T., Lackford, B., Zheng, X., Miao, Y.L., Zhou, B., Han, L., Fargo, D.C.*, et al.* (2014). INO80 facilitates pluripotency gene activation in embryonic stem cell self-renewal, reprogramming, and blastocyst development. Cell Stem Cell *14*, 575-591.
Whyte, W.A., Bilodeau, S., Orlando, D.A., Hoke, H.A., Frampton, G.M., Foster, C.T., Cowley, S.M., and Young, R.A. (2012). Enhancer decommissioning by LSD1 during embryonic stem cell differentiation. Nature *482*, 221-225.
Williams, K., Christensen, J., Pedersen, M.T., Johansen, J.V., Cloos, P.A., Rappsilber, J., and Helin, K. (2011). TET1 and hydroxymethylcytosine in transcription and DNA methylation fidelity. Nature *473*, 343-348.
Wu, H., D'Alessio, A.C., Ito, S., Wang, Z., Cui, K., Zhao, K., Sun, Y.E., and Zhang, Y. (2011). Genome-wide analysis of 5-hydroxymethylcytosine distribution reveals its dual function in transcriptional regulation in mouse embryonic stem cells. Genes Dev *25*, 679-684.
Wu, X., Johansen, J.V., and Helin, K. (2013). Fbxl10/Kdm2b recruits polycomb repressive complex 1 to CpG islands and regulates H2A ubiquitylation. Mol Cell *49*, 1134-1146.
Yildirim, O., Li, R., Hung, J.H., Chen, P.B., Dong, X., Ee, L.S., Weng, Z., Rando, O.J., and Fazzio, T.G. (2011). Mbd3/NURD complex regulates expression of 5-hydroxymethylcytosine marked genes in embryonic stem cells. Cell *147*, 1498-1510.

Ying, Q.L., Stavridis, M., Griffiths, D., Li, M., and Smith, A. (2003). Conversion of embryonic stem cells into neuroectodermal precursors in adherent monoculture. Nat Biotechnol *21*, 183-186.
Yuan, P., Han, J., Guo, G., Orlov, Y.L., Huss, M., Loh, Y.H., Yaw, L.P., Robson, P., Lim, B., and Ng, H.H. (2009). Eset partners with Oct4 to restrict extraembryonic trophoblast lineage potential in embryonic stem cells. Genes Dev *23*, 2507-2520.
Zhao, W., Li, Q., Ayers, S., Gu, Y., Shi, Z., Zhu, Q., Chen, Y., Wang, H.Y., and Wang, R.F. (2013). Jmjd3 inhibits reprogramming by upregulating expression of INK4a/Arf and targeting PHF20 for ubiquitination. Cell *152*, 1037-1050.
Zhu, W., Yao, X., Liang, Y., Liang, D., Song, L., Jing, N., Li, J., and Wang, G. (2015). Mediator Med23 deficiency enhances neural differentiation of murine embryonic stem cells through modulating BMP signaling. Development *142*, 465-476.
Zupkovitz, G., Tischler, J., Posch, M., Sadzak, I., Ramsauer, K., Egger, G., Grausenburger, R., Schweifer, N., Chiocca, S., Decker, T., and Seiser, C. (2006). Negative and positive regulation of gene expression by mouse histone deacetylase 1. Mol Cell Biol *26*, 7913-7928.